

**Enhanced multiple
charge inversion
algorithm**

S. Pfeifer et al.

This discussion paper is/has been under review for the journal Atmospheric Measurement Techniques (AMT). Please refer to the corresponding final paper in AMT if available.

A novel inversion algorithm for mobility particle size spectrometers considering non-sphericity and additional aerodynamic/optical number size distributions

S. Pfeifer¹, W. Birmili¹, A. Schladitz^{1,2}, T. Müller¹, A. Nowak³, and A. Wiedensohler¹

¹Leibniz Institute for Tropospheric Research, Permoserstraße 15, 04318 Leipzig, Germany

²Sächsisches Landesamt für Umwelt, Landwirtschaft und Geologie, August-Böckstiegel-Straße 1, 01326 Dresden Pillnitz, Germany

³Physikalisch-Technische Bundesanstalt, Bundesallee 100, 38116 Braunschweig, Germany

Received: 19 April 2013 – Accepted: 12 May 2013 – Published: 29 May 2013

Correspondence to: S. Pfeifer (pfeifer@tropos.de)

Published by Copernicus Publications on behalf of the European Geosciences Union.

Title Page

Abstract

Introduction

Conclusions

References

Tables

Figures

⏪

⏩

◀

▶

Back

Close

Full Screen / Esc

Printer-friendly Version

Interactive Discussion



Abstract

Multiple charge inversion is an essential procedure to convert the raw mobility distributions recorded by mobility particle size spectrometers, such as the DMPS or SMPS (Differential or Scanning Mobility Particle Sizers) into true particle number size distributions. In this work, we present a new multiple charge inversion algorithm with extended functionality. The algorithm can incorporate size distribution information from sensors that measure beyond the upper sizing limit of the mobility spectrometer, such as an aerodynamic particle sizer (APS), or an optical particle counter (OPC). This feature can considerably improve the multiple charge inversion result in the upper size range of the mobility spectrometer, for example, when substantial numbers of coarse particles are present. The program also yields a continuous size distribution from both sensors as an output. The algorithm is able to calculate the propagation of measurement errors, such as those based on counting statistics, into on the final particle number size distribution. As an additional aspect, the algorithm can perform all inversion steps under the assumption of non-spherical particle shape, including constant or size-dependent shape factor profiles.

1 Introduction

Mobility particle size spectrometers (Knutson and Whitby, 1975; Kousaka et al., 1985; McMurry, 2000) are widely used in aerosol science and have enjoyed broad application in both, laboratory and field studies. Rather than a true particle number size distribution, they measure an electrical particle mobility distribution. Knowing the bipolar charge distribution (Wiedensohler, 1988) and the instrument responses of the differential mobility analyser and the particle counter, it is possible to convey the electrical particle mobility distribution into the true particle number size distribution. This procedure has been called multiple charge inversion (Alofs and Balakumar, 1982; Kandlikar and Ramachandran, 1999). Surprisingly few publications are available that specify

Enhanced multiple charge inversion algorithm

S. Pfeifer et al.

Title Page

Abstract

Introduction

Conclusions

References

Tables

Figures



Back

Close

Full Screen / Esc

Printer-friendly Version

Interactive Discussion



Enhanced multiple charge inversion algorithm

S. Pfeifer et al.

Title Page

Abstract

Introduction

Conclusions

References

Tables

Figures



Back

Close

Full Screen / Esc

Printer-friendly Version

Interactive Discussion



their algorithm in detail, respectively the occupation of the matrix (e.g. Brunner, 2007). Wiedensohler et al. (2012) highlighted the need to characterize the performance of multiple charge inversion routines as part of an attempt to enhance the mutual comparability of worldwide atmospheric aerosol measurements. In their work, twelve contemporary multiple charge inversion routines showed deviations of up to 5 % with respect to the resulting particle number concentration. The deviations were attributed, among others, to different physical constants and charging probabilities used, different solutions to the matrix inversion problem, and different approaches of how to discretize, pre-process and post-process the data.

Only few inversion routines have been designed to handle size distribution information from multiple sensors. Some of our previous work highlighted, for example, the need to complement sub-micrometer mobility spectrometer information by additional super-micrometer size distribution measurements in specific atmospheric situations, such as dust plumes (Birmili et al., 2008; Schladitz et al., 2011). A lack of super-micrometer size distribution information could then lead to a drastic overestimation of the particle number size distribution in the upper size range of the mobility spectrometer. In practice, the implementation of integrative inversion routines will closely depend on the type of available instrumental parameters. Fiebig et al. (2005), for example, proposed an iterative method that is able to merge information from multiple size-selective instruments involving a differential mobility analyser.

In this work, we present the theoretical framework of a new inversion algorithm that inverts electrical particle mobility distribution from a mobility particle size spectrometer in conjunction with data from an aerodynamic particle sizer (APS) or an optical particle counter (OPC). The framework allows for a handling of non-spherical particles, with particle shape being represented either by a constant shape factor, or a size-dependent shape factor profile. As a key feature of the algorithm, we attempted to keep to an analytical solution of the multiple charge inversion problem, thus avoiding numerical iteration. Due to the underlying strict system of linear equations, we are further able to compute how measurement errors, such as those based on counting statistics,

propagate into the final particle number size distribution. The new capabilities of the algorithm are illustrated for two examples cases.

2 Theory

The measured electrical particle mobility distribution (EPMD) f^* can be written as a convolution integral of the true particle number size distribution (PNSD) f and the transfer function h on a electrical particle mobility scaled x-axis Z .¹

$$f^*(Z) = (f \cdot h)(Z) = \int_{-\infty}^{\infty} f(Z')h(Z - Z')dZ' \quad (1)$$

Vice versa, it is possible to calculate the real PNSD by the measured EPMD, by deconvolution. From the beginning, we abandon the attempt to find the direct analytic solution of the transfer function for a deconvolution. The measured EPMD is given at N discrete mobility sampling points, so the problem is transformed to a system of equations, which is easy to solve.

$$\begin{pmatrix} f_1^* \\ \vdots \\ f_N^* \end{pmatrix} = \begin{pmatrix} a_{11} & \dots & a_{1N} \\ \vdots & \ddots & \vdots \\ a_{N1} & \dots & a_{NN} \end{pmatrix} \begin{pmatrix} f_1 \\ \vdots \\ f_N \end{pmatrix} \quad (2)$$

2.1 DMA transfer function

The transfer function h^{dma} of particles through a DMA at the position Z , can be simply described by a triangular function with the height $\alpha(Z)$ and the dimensionless half-wide $\beta(Z)$, respectively the dimensionless area $A(Z) = \alpha(Z)\beta(Z)$.

¹A diameter D scaled x-axis is also possible, but not used in this work.

Enhanced multiple charge inversion algorithm

S. Pfeifer et al.

Title Page

Abstract

Introduction

Conclusions

References

Tables

Figures

◀

▶

◀

▶

Back

Close

Full Screen / Esc

Printer-friendly Version

Interactive Discussion



Ignoring multiple charged particles, the convolution integral of the DMA transfer function is:

$$f^*(Z) = \int_{-\infty}^{\infty} f(Z')h^{\text{dma}}(Z - Z')dZ' \quad (3)$$

while the transfer function (see Fig. 1) is given by Stolzenburg (1988).

$$h^{\text{dma}}(Z - Z') = \begin{cases} \frac{\alpha}{2\beta} \left(\left| \frac{Z'}{Z} - (1 + \beta) \right| + \left| \frac{Z'}{Z} + (1 + \beta) \right| - 2 \left| \frac{Z'}{Z} - 1 \right| \right) & Z' \in ((1 - \beta)Z, (1 + \beta)Z) \\ 0 & \text{else} \end{cases} \quad (4)$$

In case of an almost constant real PNSD f in the range of $(1 - \beta)Z$ and $(1 + \beta)Z$, the convolution can be approximated (Stratmann et al., 1997) by $f^*(Z) \simeq f(Z)A(Z)$. This can be rewritten, so that the transfer function of the DMA is approximately:

$$h^{\text{dma}}(Z - Z') = A(Z)\delta(Z' - Z). \quad (5)$$

It should be mentioned that under conditions of atmospheric aerosol particles the approximation is adequate, due to weak variations of the PNSD in the range of the transfer function. For narrow particle size distributions, such as generated in the laboratory, this approximation is expected to be invalid. For such conditions, it is necessary to consider also the real shape of the transfer function.

2.2 Charging probability and transfer function of multiple charged particles

To calculate the probability of multiply charged particles in a bipolar charge equilibrium, we use the analytical approximation formulae given by Wiedensohler (1988). Since we intend to consider non spherical particles in the algorithm, we employ the volume equivalent particle diameter D_{pve} as the size parameter.

This approach needs to be viewed critically, because the orientated average geometrical cross section, which is the much more important size parameter, would increase for non-spherical shapes. Wiedensohler's approximation is valid for singly and doubly charged particles smaller than 1 μm . For larger particles or higher charged particles we use the Gunn-distribution.

$$\rho(D_{\text{pve}}, n) = 10 \left[\sum_{L=0}^5 a_L(n) \left(\log \frac{D_{\text{pve}}}{\text{nm}} \right)^L \right] \quad (6a)$$

$$\rho(D_{\text{pve}}, n) = \frac{1}{\sqrt{2\pi}\sigma} \exp \left[-\frac{(n - \sigma \ln(0.875))^2}{2\sigma} \right] \quad (6b)$$

$$\sigma = \frac{2\pi\epsilon_0 D_{\text{pve}} kT}{q_{e2}}$$

$a_i(n)$ are the fit parameter of the fifth degree polynomial approximation (see Table 1).

The measured EPMD is influenced by multiple charges. That means, for a given mobility diameter a mobility particle size spectrometer detects not only single charged particle with the electrical mobility Z , but also larger, multiple charged particles with the same electrical mobility Z/n ($n = 2, 3, \dots$).

Enhanced multiple charge inversion algorithm

S. Pfeifer et al.

Title Page

Abstract

Introduction

Conclusions

References

Tables

Figures

◀

▶

◀

▶

Back

Close

Full Screen / Esc

Printer-friendly Version

Interactive Discussion



Using Eq. (6) we calculate the probability of specific multiple charges $\rho(D_{\text{pve}}, n)$. The transfer function to consider multiple charges h^{cha} is:

$$\begin{aligned}
 h^{\text{cha}}(Z - Z') &= \rho\left(D_{\text{pve}}\left(\frac{1}{1}Z\right), n=1\right) \delta\left(Z' - \frac{1}{1}Z\right) \\
 &+ \rho\left(D_{\text{pve}}\left(\frac{1}{2}Z\right), n=2\right) \delta\left(Z' - \frac{1}{2}Z\right) \\
 &+ \dots \\
 &+ \rho\left(D_{\text{pve}}\left(\frac{1}{k}Z\right), n=k\right) \delta\left(Z' - \frac{1}{k}Z\right) \\
 &+ \dots \\
 &= \sum_{n=1}^{\infty} \rho\left(D_{\text{pve}}\left(\frac{1}{n}Z\right), n\right) \delta\left(Z' - \frac{1}{n}Z\right).
 \end{aligned} \tag{7}$$

2.3 Resulting system of equations

5 The total transfer function h is the convolution of the DMA transfer function (Eq. 5) with the transfer function for multiple charged particles (Eq. 7). Because of the approximation of Stratmann et al. (1997), which implies that f has the unit $dn/d\ln Z$, we have to consider a conversion factor C_i (see Appendix A) to obtain the common unit $dn/d\log D$. We derive the complete transfer function with:

$$10 \quad h(Z - Z') = \sum_{n=1}^{\infty} \rho\left(D_{\text{pve}}\left(\frac{1}{n}Z\right), n\right) A\left(\frac{1}{n}Z\right) C_i\left(D_{\text{pve}}\left(\frac{1}{n}Z\right)\right) \delta\left(Z' - \frac{1}{n}Z\right). \tag{8}$$

Enhanced multiple charge inversion algorithm

S. Pfeifer et al.

| | |
|--------------------------|--------------|
| Title Page | |
| Abstract | Introduction |
| Conclusions | References |
| Tables | Figures |
| ◀ | ▶ |
| ◀ | ▶ |
| Back | Close |
| Full Screen / Esc | |
| Printer-friendly Version | |
| Interactive Discussion | |



Let E be the value of efficiency, by combining the probability of multiply charged particles and the DMA efficiency inclusive the conversion factor, with:

$$E(Z, n) = \rho \left(D_{\text{pve}} \left(\frac{1}{n} Z \right), n \right) A \left(\frac{1}{n} Z \right) C_i \left(D_{\text{pve}} \left(\frac{1}{n} Z \right) \right). \quad (9)$$

In case, the diffusion losses inside the LDMA as well as the CPC efficiency are not already contained in the efficiency A , they have to be added to the total efficiency E . Exemplary, in Appendix C, one can see the simple modification of the efficiency E , in case, using a cloud condensation nuclei counter (CCNC) instead of a CPC. Finally we obtain an equation for the measured electrical particle mobility size distribution at Z as a function of the real PNSD.

$$\begin{aligned} f^*(Z) &= \int_{-\infty}^{\infty} f(Z') \sum_{n=1}^{\infty} E(Z, n) \delta \left(Z' - \frac{1}{n} Z \right) dZ' \\ &= \sum_{n=1}^{\infty} E(Z, n) \int_{-\infty}^{\infty} f(Z') \delta \left(Z' - \frac{1}{n} Z \right) dZ' \\ &= \sum_{n=1}^{\infty} E(Z, n) f \left(\frac{1}{n} Z \right). \end{aligned} \quad (10)$$

As already mentioned the measured EPMD is given in N discrete mobility sampling points. Where:

$$f_i^* = f^*(Z_i) = \sum_{n=1}^{\infty} E(Z_i, n) f \left(\frac{1}{n} Z_i \right). \quad (11)$$

By using the equation of linear interpolation, given in Appendix B, we obtain:

$$f \left(\frac{1}{n} Z_i \right) = \frac{\frac{1}{n} Z_i - Z_j}{Z_{j+1} - Z_j} f_{j+1} + \frac{Z_{j+1} - \frac{1}{n} Z_i}{Z_{j+1} - Z_j} f_j \quad (12)$$

Enhanced multiple charge inversion algorithm

S. Pfeifer et al.

| | |
|--------------------------|--------------|
| Title Page | |
| Abstract | Introduction |
| Conclusions | References |
| Tables | Figures |
| ◀ | ▶ |
| ◀ | ▶ |
| Back | Close |
| Full Screen / Esc | |
| Printer-friendly Version | |
| Interactive Discussion | |



for $\frac{1}{n}Z_i \in (Z_j, Z_{j+1})$. The sampling points of the real PNSD should be identical with those of the measured EPMD. With this approach we are as close as possible to the actual information content of the measurement.

So we found the a system of equations for the multiply charge inversion with the entries of matrix **A**:

$$a_{ij} = \sum_{n=1}^{\infty} E(Z_i, n) \begin{cases} \frac{\frac{1}{n}Z_i - Z_{j-1}}{Z_j - Z_{j-1}} & \frac{1}{n}Z_i \in (Z_{j-1}, Z_j) \\ 1 & \frac{1}{n}Z_i = Z_j \\ \frac{Z_{j+1} - \frac{1}{n}Z_i}{Z_{j+1} - Z_j} & \frac{1}{n}Z_i \in (Z_j, Z_{j+1}) \\ 0 & \text{else} \end{cases} \quad (13)$$

so that:

$$\mathbf{f}^* = \mathbf{A} \cdot \mathbf{f}. \quad (14)$$

Because the number and position of the sampling points of the inverted PNSD and the measured EPMD should be identical, the matrix **A** is quadratic. Furthermore, due to $i > j \Rightarrow a_{ij} = 0$, it is a upper triangular matrix, respectively a less occupied upper triangular matrix, easy to solve with a unique solution, by e.g. simple Gauss–Jordan algorithm. Let **L** be the inverse of **A**. Finally, we obtain the solution as a system of equations.

$$\mathbf{f} = \mathbf{A}^{-1} \cdot \mathbf{f}^* = \mathbf{L} \cdot \mathbf{f}^* \quad (15)$$

2.4 Enhanced inversion

Under specific atmospheric conditions, particles outside of the measurement range of the mobility particle size spectrometer might influence the results of the multiple charge inversion. One example is the presence of significant numbers of coarse particles above the uppermost diameter channel of the mobility particle size spectrometer.

Enhanced multiple charge inversion algorithm

S. Pfeifer et al.

Title Page

Abstract

Introduction

Conclusions

References

Tables

Figures

◀

▶

◀

▶

Back

Close

Full Screen / Esc

Printer-friendly Version

Interactive Discussion



Enhanced multiple charge inversion algorithm

S. Pfeifer et al.

Title Page

Abstract

Introduction

Conclusions

References

Tables

Figures



Back

Close

Full Screen / Esc

Printer-friendly Version

Interactive Discussion



The reason is that multiply charged particles of that population will appear as particle counts that are superimposed onto the signal of particles with low charge (single and double) in the nominal mobility particle size spectrometer range.

Disturbances could only completely be avoided if a mobility spectrometer were able to measure the PNSD across the entire range until the concentration reaches zero at the upper end. Due to technical reasons, however, the range of a mobility particle size spectrometer cannot be extended far beyond 1–2 μm . In practice, the range of most mobility particle size spectrometers employed in atmospheric measurements terminates between 500 and 900 nm.

One approach has been to extrapolate the measured electrical particle mobility distribution into bigger diameters (Brunner, 2007). This might be appropriate in the case of a continuously decreasing number concentration towards larger particles, but usually not when a significant coarse particle mode is present. Therefore, information of bigger particles is needed, for example using an aerodynamic particle sizer (APS) or an optical particle counter (OPC). Schladitz et al. (2009) first proposed the approach of correcting the measured EPMD for the effect of multiple charges prior to the actual inversion. We now present an implementation of this idea into the present inversion algorithm.

If we assume that the real PNSD, we are looking for, is a composition of a PNSD f^m with N sampling points, measured with a mobility particle size spectrometer, and an additional PNSD (volume equivalent diameter) f^a (in the following named aPNSD), e.g. measured with an optical or aerodynamic particle size spectrometers, with M sampling points.

Enhanced multiple charge inversion algorithm

S. Pfeifer et al.

$$f = \begin{pmatrix} f_1^m \\ \vdots \\ f_N^m \\ f_{N+1}^a \\ \vdots \\ f_{N+M}^a \end{pmatrix}. \tag{16}$$

The additional indices m and a are added to indicate that the sampling points belong to the mobility particle size spectrometer or the aPNSD. In accordance with Eq. (11) one can calculate the measured EPMD for the first N sampling points, while the results for the aPNSD should be untouched by this algorithm.

$$f_i^* = \begin{cases} \sum_{n=1}^{\infty} E(Z_i, n) f\left(\frac{1}{n}Z_i\right) & i \leq N \\ f(Z_i) & i > N \end{cases} \tag{17}$$

In case there is an overlap of the sampling points of the both PNSDs, the function of the combined PNSD can be written as:

$$f\left(\frac{1}{n}Z_i\right) = \begin{cases} \frac{\frac{1}{n}Z_i - Z_j^m}{Z_{j+1}^m - Z_j^m} f_{j+1}^m + \frac{Z_{j+1}^m - \frac{1}{n}Z_i}{Z_{j+1}^m - Z_j^m} f_j^m & \frac{1}{n}Z_i \in (Z_j^m, Z_{j+1}^m) \wedge \frac{1}{n}Z_i \leq Z_N^m \\ \frac{\frac{1}{n}Z_i - Z_j^a}{Z_{j+1}^a - Z_j^a} f_{j+1}^a + \frac{Z_{j+1}^a - \frac{1}{n}Z_i}{Z_{j+1}^a - Z_j^a} f_j^a & \frac{1}{n}Z_i \in (Z_j^a, Z_{j+1}^a) \wedge \frac{1}{n}Z_i > Z_N^m \end{cases} \tag{18}$$

In this case, the function values of the mobility particle size spectrometers are used, as long as the multiple charged particles are in the detection range. Or in other words, in the overlap range, we use the data of mobility particle spectrometer.² It is important to assign it to the one or the other PNSD. If it is assign to both, it would be overvalued

²The reverse case, using the the aPNSD in the overlap range is also possible.

Title Page

Abstract Introduction

Conclusions References

Tables Figures

◀ ▶

◀ ▶

Back Close

Full Screen / Esc

Printer-friendly Version

Interactive Discussion



and considered wrongly twice. This overlap is useful as an indicator. If the enhanced algorithm and the measurements are correct, the inverted PNSD of the mobility particle spectrometer and the aPNSD of the optical or aerodynamic particle size spectrometer fits together.

5 The resulting matrix consists of four sub-parts:

$$a_{ij} = \begin{cases} a_{ij}^I & i \leq N \wedge j \leq N \\ a_{ij}^{II} & i \leq N \wedge j > N \\ a_{ij}^{III} & i > N \wedge j \leq N \\ a_{ij}^{IV} & i > N \wedge j > N. \end{cases} \quad (19)$$

Under these conditions, there should be an overlap range and in this range use the mobility particle size spectrometer data, the first part a_{ij}^I is identical with Eq. (13), describing the interaction of the multiple charges of the PNSD, itself.

$$10 \quad a_{ij}^I = \sum_{n=1}^{\infty} E(Z_i, n) \begin{cases} \frac{\frac{1}{n}Z_i - Z_{j-1}^m}{Z_j^m - Z_{j-1}^m} & \frac{1}{n}Z_i \in (Z_{j-1}^m, Z_j^m) \\ 1 & \frac{1}{n}Z_i = Z_j^m \\ \frac{Z_{j+1}^m - \frac{1}{n}Z_i}{Z_{j+1}^m - Z_j^m} & \frac{1}{n}Z_i \in (Z_j^m, Z_{j+1}^m) \\ 0 & \text{else.} \end{cases} \quad (20)$$

The second part a_{ij}^{II} describes the interaction of multiple charged particles of the aPNSD and the PNSD measured with the mobility particle size spectrometer.

$$a_{ij}^{II} = \sum_{n=1}^{\infty} E(Z_i, n) \begin{cases} \frac{\frac{1}{n}Z_i - Z_{j-1}^a}{Z_j^a - Z_{j-1}^a} & \frac{1}{n}Z_i \in (Z_{j-1}^a, Z_j^a) \wedge \frac{1}{n}Z_i > Z_N^m \\ 1 & \frac{1}{n}Z_i = Z_j^a \wedge \frac{1}{n}Z_i > Z_N^m \\ \frac{Z_{j+1}^a - \frac{1}{n}Z_i}{Z_{j+1}^a - Z_j^a} & \frac{1}{n}Z_i \in (Z_j^a, Z_{j+1}^a) \wedge \frac{1}{n}Z_i > Z_N^m \\ 0 & \text{else.} \end{cases} \quad (21)$$

Enhanced multiple charge inversion algorithm

S. Pfeifer et al.

Title Page

Abstract

Introduction

Conclusions

References

Tables

Figures

◀

▶

◀

▶

Back

Close

Full Screen / Esc

Printer-friendly Version

Interactive Discussion



Generally, due to the side condition for the overlap size range, the first entries of a_{ij}^{II} are empty (see Fig. 5b).

The last two parts are added to complete the rank of the matrix. Because the PNSD of the mobility particle size spectrometer has now effect on the aPNSD, a_{ij}^{III} is a zero matrix:

$$a_{ij}^{III} = 0 \quad \forall \quad i, j. \quad (22)$$

More precisely, as already mentioned, the aPNSD should be untouched, so a_{ij}^{IV} is an identity matrix:

$$a_{ij}^{IV} = 1 \quad \forall \quad i = j \quad (23)$$

$$\mathbf{A} = \begin{pmatrix} a_{11}^I & \cdots & a_{1N}^I & a_{1(N+1)}^{II} & \cdots & a_{1(N+M)}^{II} \\ \vdots & \ddots & \vdots & \vdots & \ddots & \vdots \\ a_{N1}^I & \cdots & a_{NN}^I & a_{N(N+1)}^{II} & \cdots & a_{N(N+M)}^{II} \\ a_{(N+1)1}^{III} & \cdots & a_{(N+1)N}^{III} & a_{(N+1)(N+1)}^{IV} & \cdots & a_{(N+1)(N+M)}^{IV} \\ \vdots & \ddots & \vdots & \vdots & \ddots & \vdots \\ a_{(N+M)1}^{III} & \cdots & a_{(N+M)N}^{III} & a_{(N+M)(N+1)}^{IV} & \cdots & a_{(N+M)(N+M)}^{IV} \end{pmatrix}. \quad (24)$$

Respectively, by inserting the conditions to obtain the full rank, the matrix is:

$$\mathbf{A} = \begin{pmatrix} a_{11}^I & \cdots & a_{1N}^I & a_{1(N+1)}^{II} & \cdots & a_{1(N+M)}^{II} \\ \vdots & \ddots & \vdots & \vdots & \ddots & \vdots \\ 0 & \cdots & a_{NN}^I & a_{N(N+1)}^{II} & \cdots & a_{N(N+M)}^{II} \\ 0 & \cdots & 0 & 1 & \cdots & 0 \\ \vdots & \ddots & \vdots & \vdots & \ddots & \vdots \\ 0 & \cdots & 0 & 0 & \cdots & 1 \end{pmatrix}. \quad (25)$$

Enhanced multiple charge inversion algorithm

S. Pfeifer et al.

| | |
|--------------------------|--------------|
| Title Page | |
| Abstract | Introduction |
| Conclusions | References |
| Tables | Figures |
| ◀ | ▶ |
| ◀ | ▶ |
| Back | Close |
| Full Screen / Esc | |
| Printer-friendly Version | |
| Interactive Discussion | |



Also the enhanced multiple charge matrix is a less occupied upper triangular matrix, we are able to solve:

$$\mathbf{f} = \mathbf{L} \cdot \mathbf{f}^*. \quad (26)$$

While the solution for the inverted PNSD is located in the first N entries of the vector \mathbf{f} .

2.5 Error propagation

An important, often ignored, point is to investigate the error propagation by using an inversion algorithm. As an assumption, let the measured EPMD be influenced by an error due to counting statistics of the condensation particle counter (CPC). So the values of the measured and inverted distributions can be interpreted as random variables. For the expectation value of a linear transformation Y of random a variable X it is valid:

$$E(Y) = E(aX + b) = aE(X) + b. \quad (27)$$

Additionally, for a sum of n random variables X_i it is valid:

$$E\left(\sum_{i=0}^n X_i\right) = \sum_{i=0}^n E(X_i). \quad (28)$$

As a result for the expectation value of the inverted PNSD we obtain:

$$E(\mathbf{f}) = \mathbf{L} \cdot E(\mathbf{f}^*). \quad (29)$$

For the variance of the linear transformation it is valid:

$$\text{Var}(Y) = \text{Var}(aX + b) = a^2 \text{Var}(X). \quad (30)$$

Enhanced multiple charge inversion algorithm

S. Pfeifer et al.

Title Page

Abstract

Introduction

Conclusions

References

Tables

Figures

◀

▶

◀

▶

Back

Close

Full Screen / Esc

Printer-friendly Version

Interactive Discussion



In contrast to the expectation value, for the variance of the sum of n random variables X_i , one requires the condition, that the random variables are pairwise uncorrelated, i.e. statistically independent. According to the *Bienaymé* formula it is valid:

$$\text{Var} \left(\sum_{i=0}^n X_i \right) = \sum_{i=0}^n \text{Var}(X_i). \quad (31)$$

5 Finally, for the variance of the inverted PNSD we obtain:

$$\text{Var}(\mathbf{f}) = \mathbf{L}^{\text{var}} \cdot \text{Var}(\mathbf{f}^*) \quad (32)$$

while \mathbf{L}^{var} is a matrix occupied by the squared entries of \mathbf{L} .

$$l_{ij}^{\text{var}} = l_{ij}^2 \quad \forall \quad 0 \leq i, j \leq N. \quad (33)$$

These aspects are valid either for the conventional or the enhanced inversion.

10 3 Results

We devised a system of equations that directly transforms the measured EPMD to the real PNSD. This means an improvement in many respects:

1. The presented method preserves the original size bins of the measured electrical particle mobility distribution. This avoids unnecessary interpolations of the data into new size bins and the typically associated changes in the originally measured information.
- 15 2. The operator matrix and its inverted matrix are based on linear equations. With matrix inversion accomplished, the multiple charge inversion problem reduces to a simple matrix multiplication, which is computationally very efficient if multiple EPMD having the same mobility bins are to be processed.
- 20

Enhanced multiple charge inversion algorithm

S. Pfeifer et al.

Title Page

Abstract

Introduction

Conclusions

References

Tables

Figures

⏪

⏩

◀

▶

Back

Close

Full Screen / Esc

Printer-friendly Version

Interactive Discussion



Enhanced multiple charge inversion algorithm

S. Pfeifer et al.

Title Page

Abstract

Introduction

Conclusions

References

Tables

Figures

⏪

⏩

◀

▶

Back

Close

Full Screen / Esc

Printer-friendly Version

Interactive Discussion



3. The algorithm can easily incorporate information from additional sensors measuring particles outside of the nominal measurement range of the particle mobility size spectrometer.
4. Because the inversion reduces to linear matrix multiplication, it is straightforward to compute effects of error propagation (see Sect. 2.5).
5. The algorithm can handle all procedures using a constant or size-dependent aerodynamic shape factor.

3.1 Validation of sub-micrometer EPMD inversion

We compared this inversion routine with many other inversion routines within the framework of technical harmonization of particle mobility size spectrometry (Wiedensohler et al., 2012). Figure 2 visualises the bias of our inversion routine against seven other contemporary inversion routines, on the basis of an inversion of the same sub-micrometer EPMD. It can be seen that the different methods agree within a relative deviation of 5% for a wide particle size range. Larger deviations were explained by differing interpolation methods.

3.2 Inversion of a wide size distribution combining SMPS and APS data

As already mentioned, particles outside of the measurement range of the mobility particle size spectrometer might affect the results of the sub-micrometer multiple charge inversion. In Fig. 3, we illustrate the benefits of a multiple charge inversion combining information from multiple sizing instruments, involving SMPS and APS, for the case of an atmospheric dust storm event in Morocco (Schladitz et al., 2009).

Figure 3 shows a bimodal shape of the EMPD, with number concentration maxima around 80 and 300 nm. It is worth to note that in the uppermost SMPS sampling channel (corresponding to singly charged particles of 570 nm), the EMPD drops to just half of the maximum value of the EPMD. Meanwhile, the APS size distributions reveals

Enhanced multiple charge inversion algorithm

S. Pfeifer et al.

Title Page

Abstract

Introduction

Conclusions

References

Tables

Figures

◀

▶

◀

▶

Back

Close

Full Screen / Esc

Printer-friendly Version

Interactive Discussion



the presence of a significant coarse particle mode with a volume equivalent modal diameter around 700 nm. A multiple charge inversion restricted to SMPS data only will necessarily need to interpret particle counts in the uppermost SMPS channel as singly charged particles. As can be seen in Fig. 3, such an inversion causes an artificial depression in the final size distribution around 50–150 nm as a result of applying the multiple charge inversion matrix. Also, the particle number size distribution at the upper tail of the distribution is heavily overestimated.

The quantitative consideration of the available APS data reveals that the particle counts in the uppermost SMPS channels contain, in fact, numerous multiple charges of particles beyond the SMPS measurement range. As can be seen in Fig. 3, the enhanced inversion algorithm combining the information of both sensors successfully accounts for this effect, and yields a bimodal particle number size distribution involving a fine and a coarse particle mode that is both, rather continuous and physically plausible. The particular result of the enhanced inversion algorithm depends on the specific assumptions regarding the aerodynamic particle shape factor and particle density. For the case shown in Fig. 3 we employed a coarse particle shape factor of 1.2, and a gravimetric density of 2.5 g cm^{-3} , which are realistic values for mineral dust based on the results of previous field studies.

3.3 Error propagation

The propagation of possible measurement errors from the EPMD into the final PNSD is illustrated in Fig. 4a and b. The basis is a one-hour average of ambient EPMD at the rural observation site Hohenpeissenberg, Germany.

In Fig. 4a, we assume a fictive relative uncertainty (standard deviation) of 10 % of particle number concentration measured in each channel of the EPMD, for example due to uncertainties of in the instrumental aerosol sample flow. The error bars show the 95 % confidence interval under the assumption of a log normal distributed random variable. Particles smaller than 20 nm are only influenced by single charged particles, therefore the relative standard deviation is identical to the measured data. In the range

Enhanced multiple charge inversion algorithm

S. Pfeifer et al.

Title Page

Abstract

Introduction

Conclusions

References

Tables

Figures

⏪

⏩

◀

▶

Back

Close

Full Screen / Esc

Printer-friendly Version

Interactive Discussion



from 20 to 600 nm an increase of the error of the inverted PNSD is noticeable. In this case, the error cumulates up to 15%. Sampling points larger than 600 nm are also influenced by multiple charges and one would expect also an increase of the error, but these multiple charged particles are located out of the detection range of the mobility particle size spectrometer. From this it follows that the relative standard deviation is identical with the measured values.

The same effect occurs for analysing the Poisson statistics based on experimental particle number counts for each raw concentration channel (see Fig. 4b), but not as significantly. The underlying reason is that the size range, influenced by multiple charged particles, exhibits the smallest errors, in minimum 1.3%.

The idea of the analytical error propagation is expandable in case of correlated sampling points. Errors or uncertainties for the diameters, respectively the x-values of the sampling points, will influence the matrix elements. Therefore it cannot be analyzed in the same way. To investigate this effect Monte Carlo simulations must be used, further on.

3.4 Suggested improvements and extensions

Although the given algorithm represents a flexible and state-of-the art tool, we see room for future improvements. A first issue would be the use of a uniform theory for the charging probability across the complete particle size range, especially for the enhanced inversion. A candidate would be the theory of Fuchs (1963).

The interpolations leading to Eq. (12) (Sect. 2.3) could be achieved by higher polynomial interpolation methods, possibly spline interpolation, rather than by linear interpolation. Meanwhile it must be noted that these methods have their own disadvantages, because they need proper initial and boundary conditions, and might also lead to artificial overshooting values in some places. In addition, the formula for the matrix entries (Eq. 13) would become much more complicated.

A relevant point issue is the true deconvolution of the DMA transfer function, whose finite width is ignored by the present version of the algorithm. Moreover, the width and

Enhanced multiple charge inversion algorithm

S. Pfeifer et al.

Title Page

Abstract

Introduction

Conclusions

References

Tables

Figures

⏪

⏩

◀

▶

Back

Close

Full Screen / Esc

Printer-friendly Version

Interactive Discussion



area of the DMA transfer function usually depend on particle size, especially for the highly diffusive particles in the lower range of mobility particle size spectrometers (Flagan, 1999). It is possible to calculate the analytic solution of convolution, respectively the integral, of a true triangle shape transfer function, especially under the assumption of a linear interpolated PNSD, and then determine the occupation of the matrix. Implementing these features would make this algorithm usable for very narrow PNSD, and possibly improve the results for the smaller diameter range. It needs to be mentioned, however, that the transfer matrix will become a band matrix with entries on both sides on the main diagonal, so that other, numerically more demanding algorithms will be needed to solve the system of equations.

4 Conclusions

We present the mathematical description of a multiple charge inversion algorithm for mobility particle size spectrometers, which is based on a forward transformation of the particle number size distribution (PNSD). The algorithm is based on very few approximations and interpolations, suggesting a number of advantages. Avoiding the interpolation of electrical particle mobility distributions (EPMD) onto a new grid helps conserve the original experimental information. Due to the strict nature of the system of equations, the algorithm is extremely fast. Meanwhile, we encountered no serious deviations to previous inversion routines due to these simplifications.

Furthermore, the algorithm is able to balance a signal caused by multiply charged particles outside the nominal measurement range of a mobility particle size spectrometers by using additional information collected with optical or aerodynamic particle size spectrometers. This extended functionality was shown to be particularly relevant in atmospheres with numerous coarse particles, which could be resuspended mineral dust or sea spray particles.

Finally, because of this strict linear dependency, it is possible to calculate the error propagation, due for example to instrumental uncertainty or counting statistics into

the inverted particle number size distribution. This is a frequently ignored aspect, but appears necessary to give the final particle number size distribution a statistical confidence and precision.

All aspects of the algorithm are applicable for non-spherical particles, with non-sphericity being handled through an aerodynamic particle shape factor that transforms mobility equivalent to volume equivalent diameters. This issue is particularly relevant for the enhanced inversion using information on super- μm dust particles.

Appendix A

Conversion of number size distribution

10 Transformation of $dn/d\ln Z$ to $dn/d\log D$ (respectively $dn/d\log D_{\text{pve}}$):

$$\frac{dn}{d\log D_{\text{pve}}} = \ln(10) \frac{D_{\text{pve}}}{Z} \left| \frac{dZ}{dD_{\text{pve}}} \right| \frac{dn}{d\ln Z} \quad (\text{A1})$$

while:

$$Z = \frac{n q_e}{3\pi \eta} \frac{C_c(D_{\text{pve}})}{\chi(D_{\text{pve}}) D_{\text{pve}}}. \quad (\text{A2})$$

Let C be the conversion factor for the density transformation:

$$15 \quad C(D_{\text{pve}}) = \ln(10) \frac{D_{\text{pve}}}{Z} \left| \frac{dZ}{dD_{\text{pve}}} \right| \quad (\text{A3})$$

respectively the inverse $C_i(D_{\text{pve}}) = C(D_{\text{pve}})^{-1}$, so that:

$$\frac{dn}{d\ln Z} = C_i(D_{\text{pve}}) \frac{dn}{d\log D_{\text{pve}}}. \quad (\text{A4})$$

Enhanced multiple charge inversion algorithm

S. Pfeifer et al.

Title Page

Abstract

Introduction

Conclusions

References

Tables

Figures



Back

Close

Full Screen / Esc

Printer-friendly Version

Interactive Discussion



Appendix B

Linear interpolation

The unknown real PNSD, the solution, is a continuous function, therefore we assume a linear interpolation for the given number of sampling points N .

$$f(x) = \begin{cases} f'_1(x - x_1) + f_1 & x_1 \leq x \leq x_2 \\ \vdots & \vdots \\ f'_{N-1}(x - x_{N-1}) + f_{N-1} & x_{N-1} \leq x \leq x_N \\ 0 & \text{else} \end{cases} \quad (\text{B1})$$

with:

$$f_i = f(x_i), \quad f'_i = \frac{f_{i+1} - f_i}{x_{i+1} - x_i}. \quad (\text{B2})$$

For $x \in (x_i, x_{i+1})$ we obtain the function value:

$$f(x) = \frac{x - x_i}{x_{i+1} - x_i} f_{i+1} + \frac{x_{i+1} - x}{x_{i+1} - x_i} f_i. \quad (\text{B3})$$

10 Appendix C

Multiple charge inversion with CCNC

It is valid:

$$f_i^* = f^*(Z_i) = \sum_{n=1}^{\infty} E(Z_i, n) f\left(\frac{1}{n} Z_i\right). \quad (\text{C1})$$

Using a CCNC instead of a CNC, modifies the efficiency. We need additionally the size dependent activation $a(D)$.

$$f_{Ci}^* = f^*(Z_i) = \sum_{n=1}^{\infty} E(Z_i, n) a\left(\frac{1}{n}Z_i\right) f\left(\frac{1}{n}Z_i\right) \quad (C2)$$

With $a\left(\frac{1}{n}Z_i\right) f\left(\frac{1}{n}Z_i\right) = f_C\left(\frac{1}{n}Z_i\right)$ we obtain:

$$f_C^* = \mathbf{A} \cdot f_C. \quad (C3)$$

While f_C is the real PNSD of the activated particles and f_C^* is the measured EMPD, when using a CCNC instead of a CNC.

References

- Alofs, D. J. and Balakumar, P.: Inversion to obtain aerosol size distributions from measurements with a differential mobility analyzer, *J. Aerosol Sci.*, 13, 513–527, 1982. 4736
- Birmili, W., Schepanski, K., Ansmann, A., Spindler, G., Tegen, I., Wehner, B., Nowak, A., Reimer, E., Mattis, I., Müller, K., Brüggemann, E., Gnauk, T., Herrmann, H., Wiedensohler, A., Althausen, D., Schladitz, A., Tuch, T., and Löschau, G.: A case of extreme particulate matter concentrations over Central Europe caused by dust emitted over the southern Ukraine, *Atmos. Chem. Phys.*, 8, 997–1016, doi:10.5194/acp-8-997-2008, 2008. 4737
- Brunner, J.: Particle Measurements (Size Distribution and Number) with a SMPS – Technical Basis and Evaluation Procedures, translated from “Partikelmessungen (Größenverteilung und Anzahl) mit einem SMPS – Grundlagen und Auswertverfahren”, Tech. Rep. No. 20051105, Revision 2.1, Stadt Zürich, Umwelt- und Gesundheitsschutz Zürich UGZ, Zürich, 2007. 4737, 4744
- Fiebig, M., Stein, C., Schröder, F., Feldpausch, P., and Petzold, A.: Inversion of data containing information on the aerosol particle size distribution using multiple instruments, *J. Aerosol Sci.*, 36, 1353–1372, 2005. 4737
- Flagan, R. C.: On differential mobility analyzer resolution, *Aerosol Sci. Tech.*, 30, 556–570, 1999. 4753

Enhanced multiple charge inversion algorithm

S. Pfeifer et al.

Title Page

Abstract

Introduction

Conclusions

References

Tables

Figures

◀

▶

◀

▶

Back

Close

Full Screen / Esc

Printer-friendly Version

Interactive Discussion



Enhanced multiple charge inversion algorithm

S. Pfeifer et al.

Title Page

Abstract

Introduction

Conclusions

References

Tables

Figures

◀

▶

◀

▶

Back

Close

Full Screen / Esc

Printer-friendly Version

Interactive Discussion



- Fuchs, N. A.: On the stationary charge distribution on aerosol particles in a bipolar ionic atmosphere, *Pure Appl. Geophys.*, 56, 185–193, 1963. 4752
- Kandlikar, M. and Ramachandran, G.: Inverse methods for analysing aerosol spectrometer measurements: a critical review, *J. Aerosol Sci.*, 30, 413–437, 1999. 4736
- 5 Knutson, E. O. and Whitby, K. T.: Aerosol classification by electrical mobility apparatus, theory, and applications, *J. Aerosol Sci.*, 6, 443–451, 1975. 4736
- Kousaka, Y., Okuyama, K., and Adachi, M.: Determination of particle size distribution of ultrafine aerosols using a differential mobility analyzer, *Aerosol Sci. Tech.*, 4, 209–225, 1985. 4736
- 10 McMurry, P. H.: A review of atmospheric aerosol measurements, *Atmos. Environ.*, 34, 1959–1999, 2000. 4736
- Schladitz, A., Müller, T., Kaaden, N., Maasling, A., Kandler, K., Ebert, M., Weinbruch, S., Deutscher, C., and Wiedensohler, A.: In situ measurements of optical properties at Tinfou (Morocco) during the Saharan Mineral Dust Experiment SAMUM 2006, *Tellus B*, 61, 64–78, 2009. 4744, 4750
- 15 Schladitz, A., Müller, T., Nordmann, S., Tesche, M., Groß, S., Freudenthaler, V., Gasteiger, J., and Wiedensohler, A.: In situ aerosol characterization at Cape Verde, Part 2: Parametrization of relative humidity- and wavelength-dependent aerosol optical properties, *Tellus B*, 63, 549–572, 2011. 4737
- 20 Stolzenburg, M. R.: An Ultrafine Aerosol Size Distribution Measuring System, Ph.D. thesis, University of Minnesota, 1988. 4739
- Stratmann, F., Kauffeldt, T., Hummes, D., and Fissan, H.: Differential electrical mobility analysis: a theoretical study, *Aerosol Sci. Tech.*, 26, 368–383, 1997. 4739, 4741
- Wiedensohler, A.: An approximation of the bipolar charge distribution for particles in the sub micron size range, *J. Aerosol Sci.*, 19, 387–389, 1988. 4739, 4759
- 25 Wiedensohler, A., Birmili, W., Nowak, A., Sonntag, A., Weinhold, K., Merkel, M., Wehner, B., Tuch, T., Pfeifer, S., Fiebig, M., Fjåraa, A. M., Asmi, E., Sellegri, K., Depuy, R., Venzac, H., Villani, P., Laj, P., Aalto, P., Ogren, J. A., Swietlicki, E., Williams, P., Roldin, P., Quincey, P., Hüglin, C., Fierz-Schmidhauser, R., Gysel, M., Weingartner, E., Riccobono, F., Santos, S., Gröning, C., Faloon, K., Beddows, D., Harrison, R., Monahan, C., Jennings, S. G., O’Dowd, C. D., Marinoni, A., Horn, H.-G., Keck, L., Jiang, J., Scheckman, J., McMurry, P. H., Deng, Z., Zhao, C. S., Moerman, M., Henzing, B., de Leeuw, G., Löschau, G., and Bastian, S.: Mobility particle size spectrometers: harmonization of technical standards and data

structure to facilitate high quality long-term observations of atmospheric particle number size distributions, Atmos. Meas. Tech., 5, 657–685, doi:10.5194/amt-5-657-2012, 2012. 4737, 4750, 4762

AMTD

6, 4735–4767, 2013

Enhanced multiple charge inversion algorithm

S. Pfeifer et al.

Title Page

Abstract

Introduction

Conclusions

References

Tables

Figures



Back

Close

Full Screen / Esc

Printer-friendly Version

Interactive Discussion



Enhanced multiple charge inversion algorithm

S. Pfeifer et al.

Table 1. Fit parameter for specific charge of the fifth degree polynomial approximation of Wiedensohler (1988).

| $a_i(N)$ | N | | | | |
|----------|----------|---------|---------|---------|----------|
| | -2 | -1 | 0 | +1 | +2 |
| a_0 | -26.3328 | -2.3197 | -0.0003 | -2.3484 | -44.4756 |
| a_1 | 35.9044 | 0.6175 | -0.1014 | 0.6044 | 79.3772 |
| a_2 | -21.4608 | 0.6201 | 0.3073 | 0.4800 | 62.8900 |
| a_3 | 7.0867 | -0.1105 | -0.3372 | 0.0013 | 26.4492 |
| a_4 | -1.3088 | -0.1260 | 0.1023 | 0.1544 | -5.7480 |
| a_5 | 0.1051 | 0.0297 | 0.0105 | 0.0320 | 0.5059 |

[Title Page](#)
[Abstract](#)
[Introduction](#)
[Conclusions](#)
[References](#)
[Tables](#)
[Figures](#)
[Back](#)
[Close](#)
[Full Screen / Esc](#)
[Printer-friendly Version](#)
[Interactive Discussion](#)


Enhanced multiple charge inversion algorithm

S. Pfeifer et al.

Title Page

Abstract

Introduction

Conclusions

References

Tables

Figures

◀

▶

◀

▶

Back

Close

Full Screen / Esc

Printer-friendly Version

Interactive Discussion

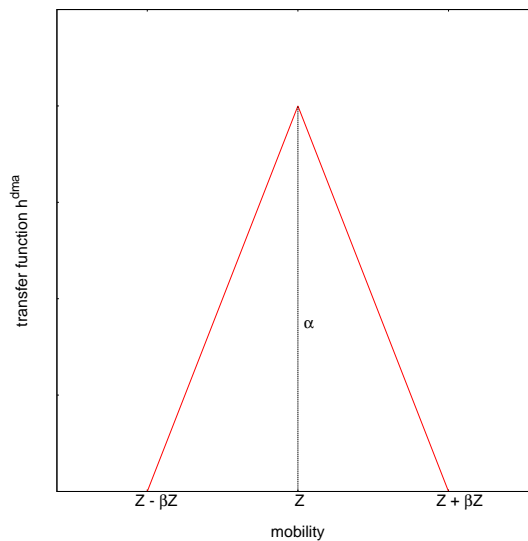


Table 2. Symbol directory.

| Symbol | Explanation |
|--------------------|---|
| D_{pve} | particle diameter (volume equivalent) |
| n | number of charges |
| $\chi(D_{pve})$ | size dependent aerodynamic shape factor |
| $Z(D_{pve}, n)$ | electrical particle mobility |
| f | real particle number size distribution (PNSD) |
| f^* | measured electrical particle mobility distribution (EPMD) |
| $\rho(D_{pve}, n)$ | charge probability |
| h^{dma} | DMA transfer function, considering the transmission |
| h^{cha} | transfer function, considering the multiple charges |
| h | total transfer function |
| $C_i(D_{pve})$ | conversion factor from $dn/d\ln Z$ to $dn/d\log D$ |
| \mathbf{A} | multiple charge matrix |
| \mathbf{L} | transformation matrix, inverse of \mathbf{A} |
| \mathbf{L}^{var} | transformation matrix of variance |

Enhanced multiple charge inversion algorithm

S. Pfeifer et al.

**Fig. 1.** Schematic of a triangular DMA transfer function.

Title Page

Abstract

Introduction

Conclusions

References

Tables

Figures

◀

▶

◀

▶

Back

Close

Full Screen / Esc

Printer-friendly Version

Interactive Discussion



Enhanced multiple charge inversion algorithm

S. Pfeifer et al.

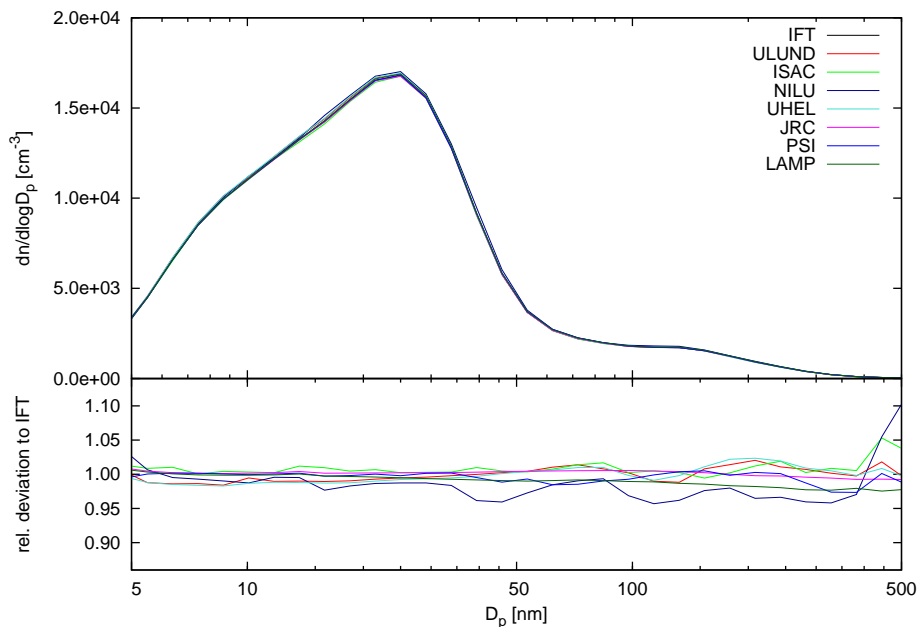


Fig. 2. Comparison of the performance of eight different multiple charge inversion routines. Shown are the different resulting PNSDs based on the very same EPMD, and their relative deviation to the new inversion routine. Reproduced from Wiedensohler et al. (2012) (IFT – Leibniz Institute for Tropospheric Research, Leipzig, Germany; ULUND – Lund University, Lund, Sweden; ISAC – Institute of Atmospheric Sciences and Climate, Bologna, Italy; NILU – Norwegian Institute for Air Research, Kjeller, Norway; UHEL – University of Helsinki, Helsinki, Finland; JRC – Joint Research Centre, Ispra, Italy; PSI – Paul Scherrer Institute, Villigen, Switzerland; LAMP – Laboratoire de Météorologie Physique, Clermont–Ferrand, France).

Title Page

Abstract

Introduction

Conclusions

References

Tables

Figures

◀

▶

◀

▶

Back

Close

Full Screen / Esc

Printer-friendly Version

Interactive Discussion



Enhanced multiple charge inversion algorithm

S. Pfeifer et al.

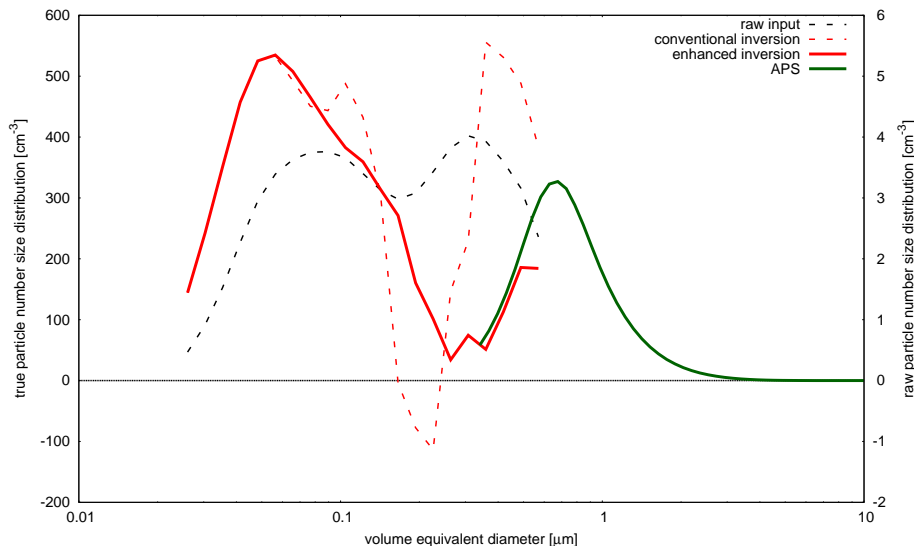


Fig. 3. Results of the particle number size distribution (PNSD) obtained from multiple charge inversion with different degrees of functionality. Dashed black line: raw electrical particle mobility distribution (EPMD). Solid green line: aerodynamic particle size distribution (APS). Red dashed line: multiple charge inversion using only SMPS data. Red solid line: enhanced multiple charge inversion combining APS and SMPS data.

[Title Page](#)[Abstract](#)[Introduction](#)[Conclusions](#)[References](#)[Tables](#)[Figures](#)[◀](#)[▶](#)[◀](#)[▶](#)[Back](#)[Close](#)[Full Screen / Esc](#)[Printer-friendly Version](#)[Interactive Discussion](#)

Enhanced multiple charge inversion algorithm

S. Pfeifer et al.

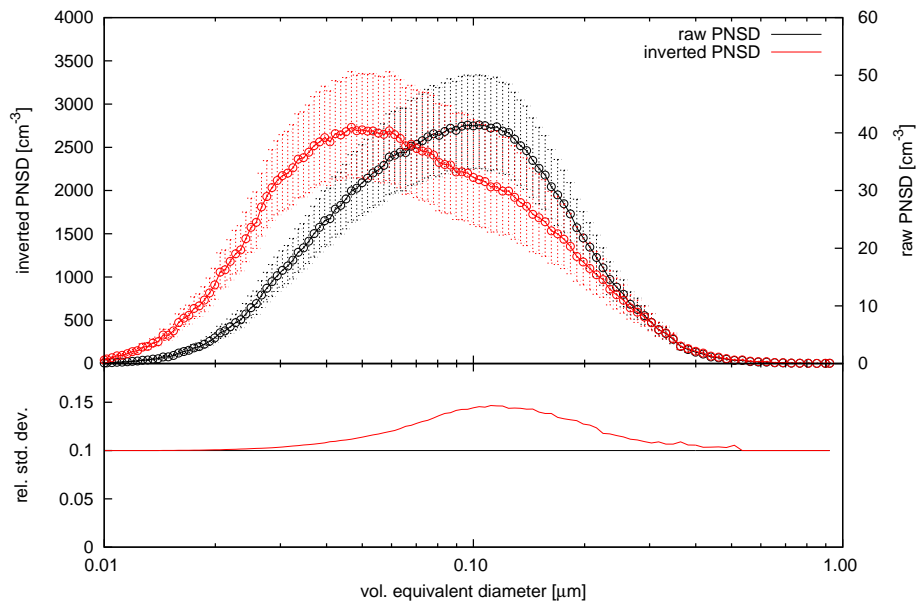


Fig. 4a. Example of the error propagation of a mobility particle size spectrometer PNSD, Hohenpeissenberg, 23 February 2012, one-hour average 00:00–01:00 LT. The fictive relative error of the results increases for sampling points influenced by charge from 10 to 15 %.

Title Page

Abstract

Introduction

Conclusions

References

Tables

Figures

◀

▶

◀

▶

Back

Close

Full Screen / Esc

Printer-friendly Version

Interactive Discussion



Enhanced multiple charge inversion algorithm

S. Pfeifer et al.

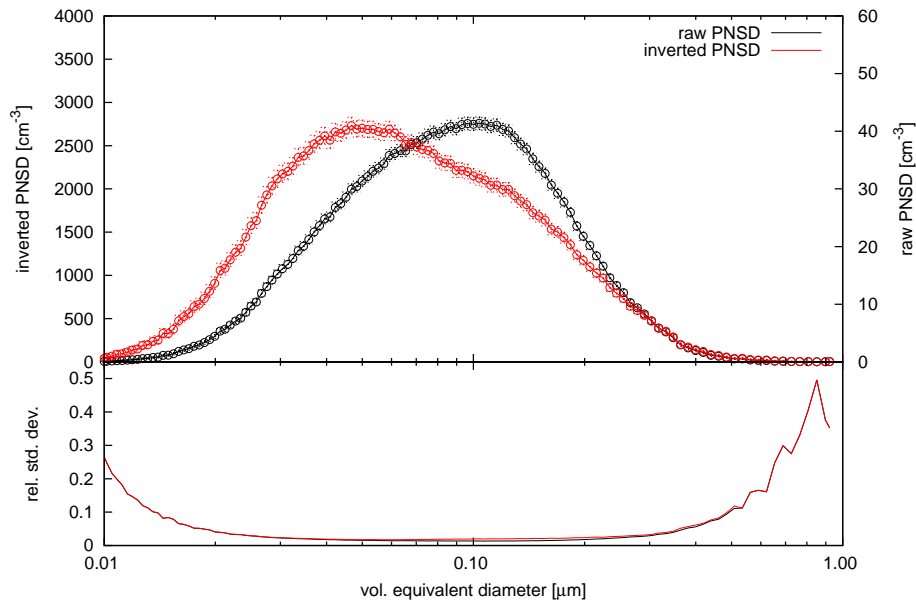


Fig. 4b. Example of the error propagation of a mobility particle size spectrometer PNSD, Hohenpeissenberg, 23 February 2012, one-hour average 00:00–01:00 LT. The relative error of the result is not significantly different from the input in case of Poisson counting statistic.

Title Page

Abstract

Introduction

Conclusions

References

Tables

Figures

◀

▶

◀

▶

Back

Close

Full Screen / Esc

Printer-friendly Version

Interactive Discussion



Enhanced multiple charge inversion algorithm

S. Pfeifer et al.

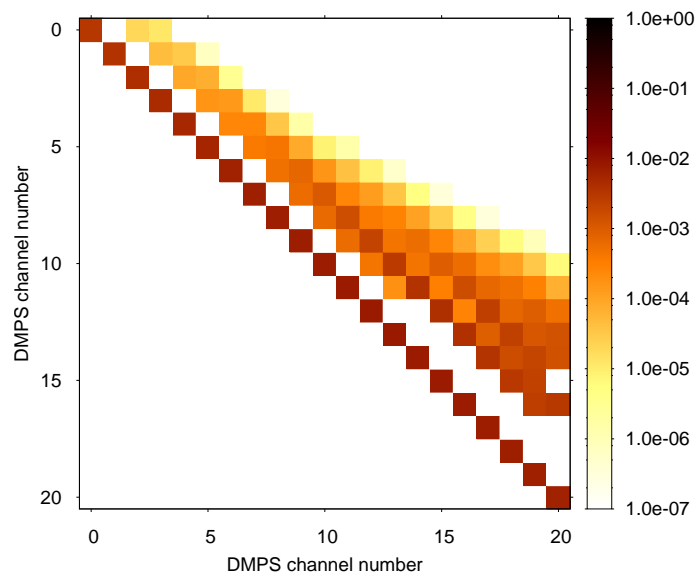


Fig. 5a. Visualization of the multiple charge matrix using only mobility particle size spectrometer data.

[Title Page](#)[Abstract](#)[Introduction](#)[Conclusions](#)[References](#)[Tables](#)[Figures](#)[◀](#)[▶](#)[◀](#)[▶](#)[Back](#)[Close](#)[Full Screen / Esc](#)[Printer-friendly Version](#)[Interactive Discussion](#)

Enhanced multiple charge inversion algorithm

S. Pfeifer et al.

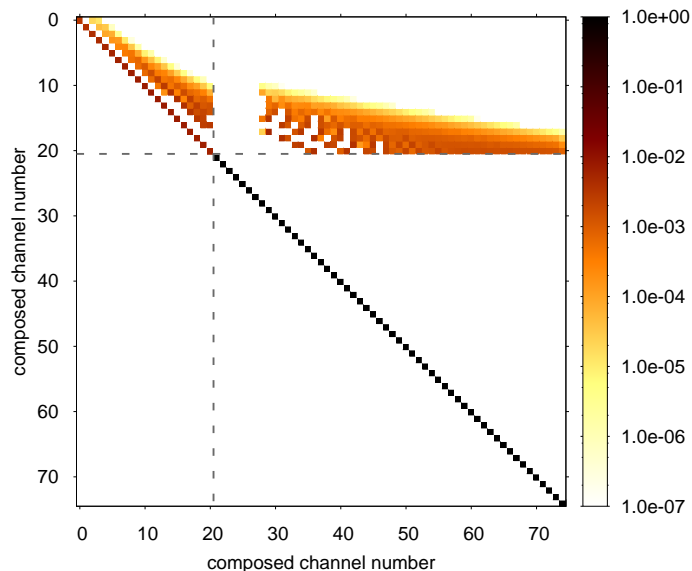


Fig. 5b. Visualization of the multiple charge matrix for the enhanced case. The first quadrant corresponds to the matrix entries shown in Fig. 5a. The second quadrant describes the charge correction of the EPMD of the mobility particle size spectrometer with information from additional sensors such as an APS or OPC. The gap for the first entries of the second quadrant is due to the finite overlap of both sizing sensors.

[Title Page](#)[Abstract](#)[Introduction](#)[Conclusions](#)[References](#)[Tables](#)[Figures](#)[⏪](#)[⏩](#)[◀](#)[▶](#)[Back](#)[Close](#)[Full Screen / Esc](#)[Printer-friendly Version](#)[Interactive Discussion](#)